

# Shadow Detection and Radiometric Restoration in Satellite High Resolution Images

Pooya Sarabandi<sup>1</sup>, Fumio Yamazaki<sup>2</sup>, Masashi Matsuoka<sup>3</sup>, Anne Kiremidjian<sup>4</sup>

<sup>1</sup>Department of Civil and Environmental Engineering, Stanford University, USA. [psarabandi@stanford.edu](mailto:psarabandi@stanford.edu)

<sup>2</sup>Department of Urban Environment Systems, Faculty of Engineering, Chiba University, Japan. [yamazaki@tu.chiba-u.ac.jp](mailto:yamazaki@tu.chiba-u.ac.jp)

<sup>3</sup>Earthquake Disaster Mitigation Research Center (EDM), Kobe, Japan. [matsuoka@edm.bosai.go.jp](mailto:matsuoka@edm.bosai.go.jp)

<sup>4</sup>Department of Civil and Environmental Engineering, Stanford University, USA. [ask@stanford.edu](mailto:ask@stanford.edu)

**Abstract**—In this paper a new transformation which enables us to detect boundaries of cast shadows in high resolution satellite images is introduced. The transformation is based on color invariant indices. Different radiometric restoration techniques such as Gamma Correction, Linear-Correlation Correction and Histogram Matching are introduced in order to restore the brightness of detected shadow area.

**Keywords**--shadow detection; radiometric restoration; invariant color indecies; texture analysis; gamma correction; linear-correlation correction; histogram matching.

## I. INTRODUCTION

In almost all cases, optical satellite images are contaminated with shadow. In order to perform a successful change detection using time series of images or to use a single image and extract information from it, it is important to identify shadow areas in the image and radiometrically restore their brightness.

Cast shadows in optical images result form the light source being blocked by objects and therefore, parts of the image are not illuminated by the direct light. These regions are usually among the darkest areas in an image and can be easily misclassified as other dark objects such as water. Using a single band of data (panchromatic image) usually does not give us enough information to distinguish between shadows and other dark objects; therefore, we use multi-band information in order to discriminate between shadow regions and other dark areas in multi-band high-resolution satellite images. We use a set of color invariant indices (as will be described in the following sections) in order to apply a non-linear transformation to our data and disaggregate the dark regions. To detect the boundaries of shadows in the image, the variance measure is used as a local statistic for the texture filter. This particular type of texture filter enables us to highlight sudden changes between shadow and non-shadow pixels at the boundary of these two regions.

Radiometric restoration of detected shadow regions can then be done using finer resolution panchromatic images. Three different restoration techniques have been introduced and results are compared for a test-region. These algorithms are: Gamma Correction Method, Linear-Correlation Method and Histogram Matching Method.

The two high-resolution satellite images investigated in this research include:

- 1- *IKONOS* images of Bhuj, India with four-meter spatial resolution in multi-spectral bands, one-meter spatial resolution in panchromatic band and 11-bit dynamic range.
- 2- *QuickBird* images of Boumerdes, Algeria with 2.4 meter spatial resolution in multi-spectral bands, 0.6 meter spatial resolution in panchromatic band and 11-bit dynamic range.

The availability of different resolutions and spectra for these images make them particularly suitable candidates for application of the algorithm developed in the study. Ideally, the panchromatic and multi-spectral images should have the same resolution. However, since such images were not available to the authors, the images listed above were used.

## II. SHADOW DETECTION

### A. Color Invariant Indecies

As stated earlier, using single band information to classify shadow regions may lead to false detections; therefore, it is desirable to employ the information available in different bands of a multi-spectral image to increase the classification's accuracy. Among many color spaces that are invariant to shadow (i.e., convey the spectral or color characteristics of image features, regardless of variations in scene illumination condition [1]) such as Hue-Saturation-Value (*HSV*) or ratio of red (R), green (G), and blue (B) bands (given as  $R/G$ ,  $G/B$  and  $B/R$ ), it was determined that the color space  $C_1 C_2 C_3$  introduced in [2] can be used as the best non-linear transformation for the purpose of shadow detection. These indices are defined as following:

$$C_1 = \arctan\left(\frac{G}{\max(R, B)}\right) \quad (1)$$

$$C_2 = \arctan\left(\frac{G}{\max(R, B)}\right) \quad (2)$$

$$C_3 = \arctan\left(\frac{B}{\max(R, G)}\right) \quad (3)$$

where  $R$ ,  $G$ , and  $B$  correspond to red, green and blue values of each pixel in the image.

Fig. 1 shows the true-color image of Bhuj, India from IKONOS satellite. Fig. 2 shows the same image after the  $C_1$ ,  $C_2$ , and  $C_3$  transformations are applied. These images are used in the next section to identify the shadow boundaries.

### B. Shadow Classification

In order to identify shadow boundaries and the region inside those boundaries, we use the third transformed channel ( $C_3$ ) and apply a  $3 \times 3$  texture-filter to compute the local variance at the neighborhood of each pixel. The variance filter can be defined as following:

$$\text{var} = \frac{1}{N} \sum_{i=0}^{N-1} \sum_{j=0}^{N-1} [f(i, j) - \bar{f}(i, j)]^2 \quad (4)$$

$$\text{where: } \bar{f}(i, j) = \frac{1}{N} \sum_{i=0}^{N-1} \sum_{j=0}^{N-1} f(i, j)^2$$

A high variance in Digital Number ( $DN$ ) is observed when there is a sharp transition from shadow to non-shadow pixels at the boundary. The resultant is an image with boundaries of shadow regions as shown in Fig. 3.



Figure 1. False-Color, IKONOS image of Bhuj

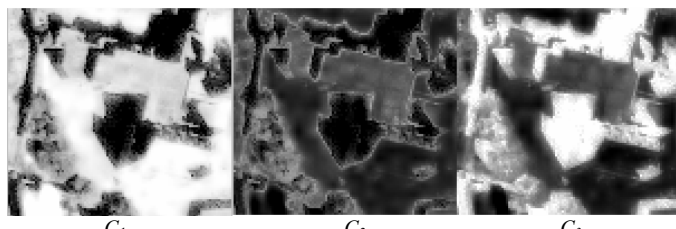


Figure 2.  $C_1C_2C_3$  Transformation on IKONOS image of Bhuj

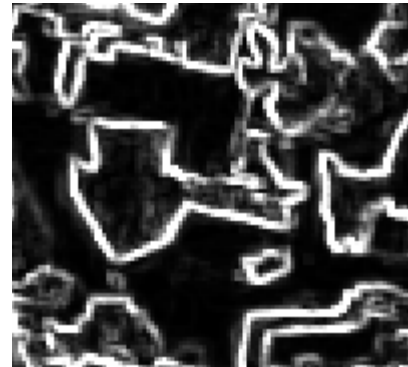


Figure 3. Shadow Boundaries Resulted from Applying Texture Filter on the Third Channel ( $C_3$ )

### III. RADIOMETRIC RESTORATION

Three different algorithms are introduced in order to radiometrically restore the detected shadow areas. These algorithms are: Gamma Correction Method, Linear-Correlation Method and Histogram Matching Method. Training data-sets are extracted from the image in order to calibrate the parameters of these algorithms. These parameters should be used for similar regions in the image and should not be applied to the entire image indiscriminantly. For example, if we calibrate our parameters for the cast shadow of buildings on bare-soil, we have to use them only in other areas where buildings cast shadows on bare-areas and not on other objects.

#### A. Gamma Correction

The gamma correction considers the shadow as a multiplicative noise source that corrupts the brightness of the underlying pixels. Therefore, we can introduce the recovered  $DN$  values of the shadow regions as given by Eq. 6:

$$DN_{\text{recovered}} = (DN_{\text{shadow}})^{\frac{1}{\gamma}} \quad (6)$$

where  $\gamma$  is the parameter of the algorithm determined from the training data set.

In practice  $DN$  values should be normalized, thus, in case of an image with 11-bit dynamic range, Eq. 6 can be written as:

$$\left(\frac{DN_{\text{recovered}}}{2047}\right) = \left(\frac{DN_{\text{shadow}}}{2047}\right)^{\frac{1}{\gamma}} \quad (7)$$

The parameter  $\gamma$  should be applied only to the class for which it is computed. To estimate the  $\gamma$  coefficient, the mean value of shadow pixels and the mean value of neighboring non-shadow pixels that are known to represent the shadow pixels are used.

#### B. Linear-Correlation Correction

If the shadow is modeled as a combination of additive and multiplicative noise, the brightness of shadow pixels to the first order can be restored by a linear function. Using the minimum square error criterion, we can define this linear function as given in Eq. 8:

$$DN_{recovered} = \frac{\sigma_{non-shadow}}{\sigma_{shadow}} (DN_{shadow} - \mu_{shadow}) + \mu_{nonshadow} \quad (8)$$

where  $\mu$  is the mean value and  $\sigma$  is the standard deviation of the shadow or non-shadow region.

The same considerations described previously about case-wise application of correction functions should be taken into account.

#### A. Histogram Matching

Histogram matching is one the classical methods that used in order to bring brightness distribution of two given images as close as possible to each other. The proposed method in [3] is used to recover the  $DN$  values of the shadow-covered pixels by matching the histogram of the shadow regions to the histogram of the non-shadow areas of the same class. This operation is sensitive to the window size in which the histograms are matched. The Quad-tree partitioning proposed in [4] is applied in order to automatically select the appropriate window sizes.

## II. RESULTS OF IMAGE RESTORATION

The QuickBird image of Boumerdes, Algeria (Fig. 4) is selected to test the algorithms described in the previous sections. Shadows in the original image are first identified by the suggested method in Section II using the multi-spectral 2.4 meter resolution image and then the image is up-sampled to a resolution of 0.6 meter using bi-cubic interpolation. The resulting shadow mask is applied to the Panchromatic image of the same area. Figures 5 through 7 show the Gamma Correction, Linear-Correlation Correction and Histogram Matching techniques applied to restore the brightness of shadow regions of the image. A smoothing filter is also applied in order to reduce the discontinuity between the restored regions and the rest of the image.

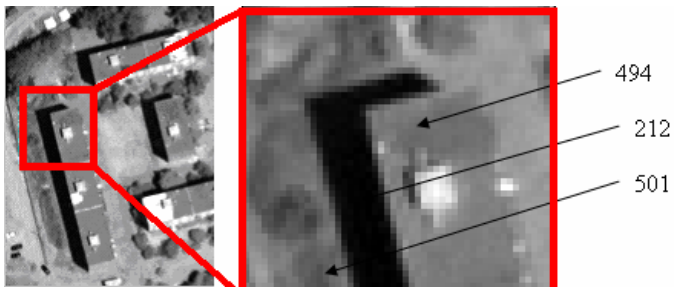


Figure 1. Panchromatic 0.6m, QuickBird image of Boumerdes, Algeria

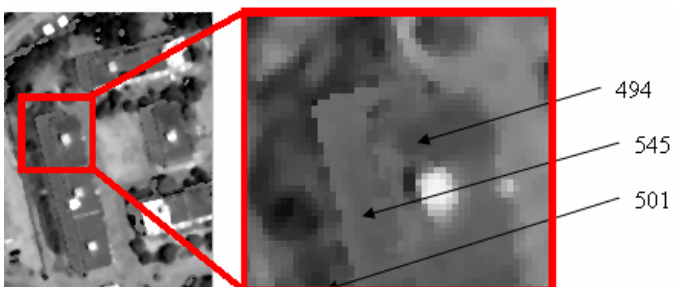


Figure 2. Gamma Correction

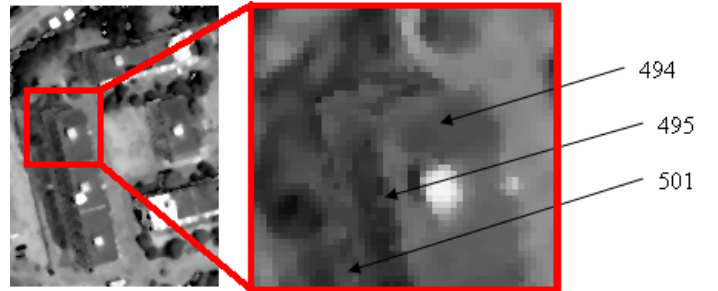


Figure 3. Linear-Correlation Correction

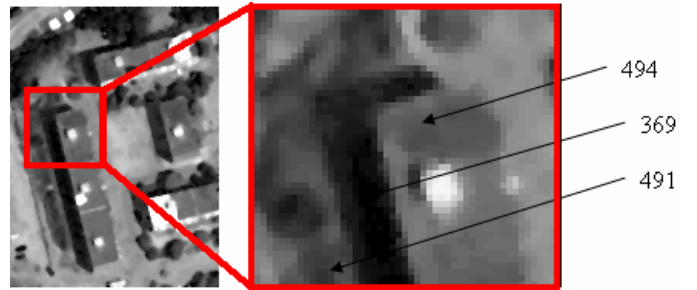


Figure 4. Histogram Matching

Table 1 summarizes sample results of application of different restoration schemes on the Panchromatic image of Boumerdes, Algeria. The presented values in Table 1 are mean  $DN$  values of each class. It can be seen that the Linear-Correlation Correction method restores  $DN$  values of shadow areas better than other techniques. The restored  $DN$  values (by Linear-Correlation method) are closer to the expected values represented by the surrounding bare-ground pixels. Gamma Correction and Histogram Matching Correction are also capable of performing radiometric restoration but not as good as Linear-Correlation Correction scheme.

TABLE I. RESULTS OF DIFFERENT RESTORATION TECHNIQUES

Correction Method	Roof $DN$ Value	Shadow $DN$ Value	Bare Ground $DN$ Value
Original	494	212	501
Gamma	494	545	501
Linear-Correlation	494	495	501
Histogram Matching	494	369	501

## III. CONCLUSION

One of the applications of shadow restoration is in change detection problems. Comparing two high-resolution registered temporal-images for the purpose of change detection often can lead to false predictions because of the existence of shadows in one image at a given location but not in the second image.

The proposed non-linear transformation  $C_1C_2C_3$  provides a color invariant space which is sensitive to shadow and is able to discriminate between shadow and other dark objects in the image. The best result for shadow classification is observed using the third dimension of this space ( $C_3$ ). By applying texture-filters (such as variance) or edge detector filters the shadow boundaries in the image can be identified. The proposed method uses multi-band rather than single-band information. This approach is an improvement over other methods that use single band information and often missrepresent shadow regions.

From the application of the shadow restoration methods presented, the best results are obtained using the Linear-Correlation Correction method. The Gamma Correlation and Histogram Matching are also able to restore the shadow brightness, but are not as effective as the Linear-Correlation method.

#### ACKNOWLEDGMENT

This research was initiated during the summer of 2003 when Mr. Sarabandi spent an internship at the Earthquake Disaster Mitigation Center in Kobe, Japan with the joint sponsorship of the National Science Foundation and the Japan Society for the Promotion of Science. The research was also supported through UPS Grant through Stanford University. The authors express their gratitude to all of these organizations for their support.

QuickBird images of Boumerdes used in this study were licensed and provided by Earthquake Engineering Research Institute, Oakland, California.

#### REFERENCES

- [1] Thomas M. Lillesand and Ralph W. Kiefer, “*Remote Sensing and Image Interpretation*”, Fourth Ed., John Wiley & Sons, 2000.
- [2] T. Gevers and A. W. M. Smeulders, “Color-based object recognition, pattern recognition”, pp. 453–464, 1999.
- [3] John A. Richards and Xiuping Jia, “*Remote Sensing Digital Image Analysis: An Introduction*”, third Ed., Springer-Verlag, Berline, 1999.
- [4] Victor J.D. Tsai, “Automatic Shadow Detection and Radiometric Restoration on Digital Aerial Images”, *IGARSS 2003*, 2003.